

UC Davis

UC Davis Previously Published Works

Title

High resolution genetic dissection of the major QTL for tipburn resistance in lettuce, *Lactuca sativa*

Permalink

<https://escholarship.org/uc/item/2zx012rd>

Journal

G3: Genes, Genomes, Genetics, 11(7)

ISSN

2160-1836

Authors

Macias-González, Miguel
Truco, Maria Jose
Han, Rongkui
[et al.](#)

Publication Date



2021-07-14

DOI

10.1093/g3journal/jkab097

Peer reviewed

High-resolution genetic dissection of the major QTL for tipburn resistance in lettuce, *Lactuca sativa*

Miguel Macias-González,^{1,2,†} Maria Jose Truco,¹ Rongkui Han ¹, Sylvie Jenni,³ and Richard W. Michelmore ^{1,2,*}

¹The Genome Center, University of California, Davis, Davis, CA 95616, USA

²Department of Plant Sciences, University of California, Davis, Davis, CA 95616, USA

³Science and Technology Branch, Agriculture and Agri-Food Canada, Saint-Jean-sur-Richelieu, QC J3B 3E6, Canada

*Corresponding author: Department of Plant Sciences, The Genome Center, University of California, Davis, Davis, CA 95616, USA. rwichelmore@ucdavis.edu

[†]Present address: United Genetics Seeds Co. 8000 Fairview Road, Hollister, CA 95023, USA.

Abstract

Tipburn is an important physiological disorder of lettuce, *Lactuca sativa* L., related to calcium deficiency that can result in leaf necrosis and unmarketable crops. The major quantitative trait locus (QTL), *qTPB5.2*, can account for up to 70% of the phenotypic variance for tipburn incidence in the field. This QTL was genetically dissected to identify candidate genes for tipburn by creating lines with recombination events within the QTL and assessing their resistance to tipburn. By comparing lines with contrasting haplotypes, the genetic region was narrowed down to ~877 Kb that was associated with a reduction of tipburn by ~60%. Analysis of the lettuce reference genome sequence revealed 12 genes in this region, one of which is a calcium transporter with a single nucleotide polymorphism in an exon between haplotypes with contrasting phenotypes. RNA-seq analysis of recombinants revealed two genes that were differentially expressed between contrasting haplotypes consistent with the tipburn phenotype. One encodes a Teosinte branched1/Cycloidea/Proliferating Cell factor transcription factor; however, differential expression of the calcium transporter was detected. The phenotypic data indicated that there is a second region outside of the ~877 Kb region but within the QTL, at which a haplotype from the susceptible parent decreased tipburn by 10–20%. A recombinant line was identified with beneficial haplotypes in each region from both parents that showed greater tipburn resistance than the resistant parent; this line could be used as the foundation for breeding cultivars with more resistance than is currently available.

Keywords: candidate genes; calcium deficiency; physiological disorder; tipburn resistance; genetic markers

Introduction

Tipburn, an important physiological disorder of lettuce (*Lactuca sativa* L.), is thought to be related to inadequate levels of calcium during leaf development and can cause growers to lose entire fields of the crop (Barta and Tibbitts 1991, 2000; Olle and Bender 2009). Packing companies can refuse a lettuce crop if tipburn incidence is over 5% (Jenni et al. 2013). Tipburn manifests as necrotic lesions at the margins of young expanding leaves (Barta and Tibbitts 1991, 2000). In iceberg-type lettuce, this damage can be localized to the younger leaves inside the head, while the exterior leaves look healthy, making it difficult to detect. Tipburn can develop despite sufficient calcium in the soil (Hartz et al. 2007); therefore, it cannot be managed by soil amendments. Foliar calcium applications may not prevent the occurrence of tipburn under field conditions (Holtshulze 2005).

Environments that are conducive to tipburn are the same as those that reduce transport of calcium to the expanding leaves. These environments can be placed into two groups (Jenni et al. 2013): (1) those that reduce the supply of calcium to leaves and (2) those that increase the demand for calcium. The first group includes environments that have high relative humidity (Choi and Lee 2008), natural or artificial enclosure of leaves (Barta and

Tibbitts 1991), and low air movement (Frantz et al. 2004). The second group includes environments that speed up plant growth such as high temperatures (Misaghi and Grogan 1978) and high fertilization (Brumm and Schenk 1993). Most of these conditions that are conducive to tipburn cannot be controlled by the grower and some are even desirable, such as the enclosed leaves of iceberg-type lettuce.

Resistance to tipburn is an important trait for lettuce cultivars (cvs.). Lettuce cvs. that are resistant to tipburn can produce crops with no or marketable levels of tipburn (Ryder and Waycott 1998; Olle and Bender 2009); however, even the most resistant cvs. succumb to tipburn when exposed to highly conducive conditions. Genetic studies on tipburn suggested that resistance is a heritable trait in lettuce that could be improved by breeding (Ryder and Waycott 1998; Jenni and Hayes 2010; Macias-González et al. 2019). Analysis of the genetics of tipburn could elucidate the causal genes for resistance to tipburn, which could be used as genetic markers to assist in breeding for resistant cvs. Jenni et al. (2013) identified a major quantitative trait locus (QTL) for tipburn incidence, *qTPB5.2*, in linkage group (LG) 5 of the reference map (Truco et al. 2013) that explained 38–70% of the variance for tipburn incidence in multiple environments and crop maturities. Macias-González et al. (2019) validated *qTPB5.2* and identified a

Received: November 11, 2020. Accepted: March 21, 2021

© The Author(s) 2021. Published by Oxford University Press on behalf of Genetics Society of America.

This is an Open Access article distributed under the terms of the Creative Commons Attribution-NonCommercial-NoDerivs licence (<http://creativecommons.org/licenses/by-nc-nd/4.0/>), which permits non-commercial reproduction and distribution of the work, in any medium, provided the original work is not altered or transformed in any way, and that the work is properly cited. For commercial re-use, please contact journals.permissions@oup.com

second major QTL in LG 1, *qTBIN_1_QC11*. Therefore, the *qTPB5.2* and *qTBIN_1_QC11* regions are targets for the identification of genes controlling tipburn.

Lettuce is amenable to genetic studies. It is diploid, can produce at least two generations per year, is self-compatible allowing the generation of homozygous lines, and produces thousands of dry seeds from a single plant. Many genetic markers have been developed and a high-quality reference genome assembly is available (Truco *et al.* 2007, 2013; Stoffel *et al.* 2012; Reyes-Chin-Wo *et al.* 2017). It is possible to screen thousands of offspring from a single generation to saturate target genomic regions with recombinants and to identify polymorphisms that can be placed relative to phenotypic variation and annotated genes in the reference genome.

In this study we dissected the major QTL, *qTPB5.2*, to identify candidate genes for tipburn incidence and provide tightly linked molecular markers for assisting breeding for tipburn resistance. Lines were created with recombination events within the QTL; these were genotyped across the QTL region and assessed for their resistance to tipburn in multiple field trials over several years. Haplotype comparisons narrowed the focus to a small region that contained few candidate genes. RNA-seq analysis revealed two genes that were differentially expressed between contrasting haplotypes consistent with the tipburn phenotype. In addition, phenotypic data suggested that a second region within the major QTL can decrease tipburn with the resistant haplotype coming from the susceptible parent. A recombinant haplotype was identified that combined beneficial haplotypes from both parents, which had greater tipburn resistance than the more resistant parent.

Materials and methods

Development of populations for fine mapping

The F_7 recombinant inbred line termed RIL 39, derived from a cross between cvs. Emperor x El Dorado (Jenni *et al.* 2013), was identified as heterozygous within intervals 1 and 2, which represented half of the target QTL on LG 5, while being homozygous for the rest of the genome, including other unlinked QTLs for tipburn resistance (Macias-González *et al.* 2019; Figure 1). Progeny from RIL 39 were genotyped and lines homozygous for contrasting haplotypes within intervals 1 and 2 (nine with the cv. Emperor haplotype and nine with the cv. El Dorado haplotype) were selected and selfed to provide seed to test in the field. The seed from these progenies were direct seeded at the University of Arizona Yuma Agricultural Center (YAC) for field evaluation in March 2014 (Supplementary Table S1).

No F_7 RILs from the same cross were heterozygous for the other half of the targeted QTL on LG 5. Therefore, RIL 85, which had the El Dorado haplotype for the region containing the target QTL and cv. Emperor haplotypes at the minor QTLs for tipburn in LGs 2 and 5 (Jenni *et al.* (2013); Macias-González *et al.* 2019), was backcrossed to cv. Emperor to produce BC_1 individuals that were heterozygous for the targeted QTL on LG 5. BC_1 individuals were then selfed and ~1500 BC_1S_1 individuals were genotyped to identify recombinants within the QTL within intervals 3–5. Ninety-six BC_1S_1 recombinant individuals were selected (Supplementary Table S2) and selfed to produce enough BC_1S_2 seed for evaluation in the field. The trial was direct seeded at YAC on December 10, 2014 and evaluated for tipburn in March 2015 (Supplementary Table S1). Based on the results of this experiment, BC_1S_2 individuals with a recombination event within interval 4 were genotyped with additional interstitial markers to identify recombinants

within this interval. The 2015 field phenotypic data from these individuals were re-analyzed with the new genotypic data. Based on these results, BC_1S_2 individuals with recombination events within intervals 4.2–4.5 were selected, which were homozygous for recombination events across the targeted region; these BC_1S_2 individuals were selfed to provide enough seed for evaluation at YAC in spring 2016 and Spence United States Department of Agriculture, Agricultural Research Service, Salinas, California (SAL) in summer 2016.

Field experiments and horticultural practices

All experiments were randomized complete block designs with four or five replications (Supplementary Table S1). The YAC 2013–2014 experiment was evaluated on March 25, 2014, at which time cv. El Dorado had hard, solid, mature heads and cv. Emperor was over-mature with some heads that were bursting. The YAC 2014–2015 experiment was evaluated on March 31, 2015, when heads of both cvs. Emperor and El Dorado were hard and over-mature. The YAC 2015–2016 experiment was scored on March 30 or April 17; tipburn evaluations were done when plants had hard, solid, mature heads. In the SAL 2016 experiment, all lines were scored twice on July 14 and 21 to evaluate tipburn at different stages of maturity. At the first scoring, cvs. Emperor and El Dorado were at acceptable market maturity with firm, compact heads that yielded slightly to moderate pressure. At the second scoring, cv. El Dorado had mature, hard heads that yielded slightly to strong pressure, whereas cv. Emperor was slightly overmature with harder, solid heads that did not yield to pressure.

Phenotyping

All experiments were evaluated for tipburn incidence. In total, 6–20 plants were evaluated per replicate depending on the experiment. For the SAL 2016 experiment, six heads were evaluated, each at two timepoints (65 and 71 days after imbibition, dai). Tipburn incidence was measured by counting the number of plants with tipburn symptoms of any severity out of the total number of plants scored.

The YAC 2015–2016 and SAL 2016 experiments were also evaluated for leaf crinkliness at the margin of leaves, average plant weight, head firmness, and tipburn severity as described in Macias-González *et al.* (2019). Leaf crinkliness was evaluated on a scale from 1 to 3, where 1 was the leaf crinkliness of cv. El Dorado and 3 was that of cv. Emperor (Supplementary Figure S3), with a score of 2 being intermediate. To evaluate average plant weight, 6 or 10 plants (depending on the experiment) were weighed before being evaluated for tipburn. To evaluate head firmness, plants were scored as described in Jenni *et al.* (2013).

Phenotypic data analysis

Data analysis was conducted using R software for statistical computing (R Core Team 2019). Analysis for tipburn incidence was conducted using the MCMCgmm package (Hadfield 2010). The haplotype was considered a fixed effect, replication was included as random effects, the intercept was removed from the model (i.e., adding -1 to the fixed effect model), and the distribution family was set to “multinomial2.” In models that had complete separation due to some lines having 100% tipburn incidence for all replications, flat priors were given to the variance matrix of the fixed effects by multiplying the diagonal matrix by $\pi^{(2/3)} + 1$. Convergence diagnostics were conducted using the coda package (Plummer 2006).

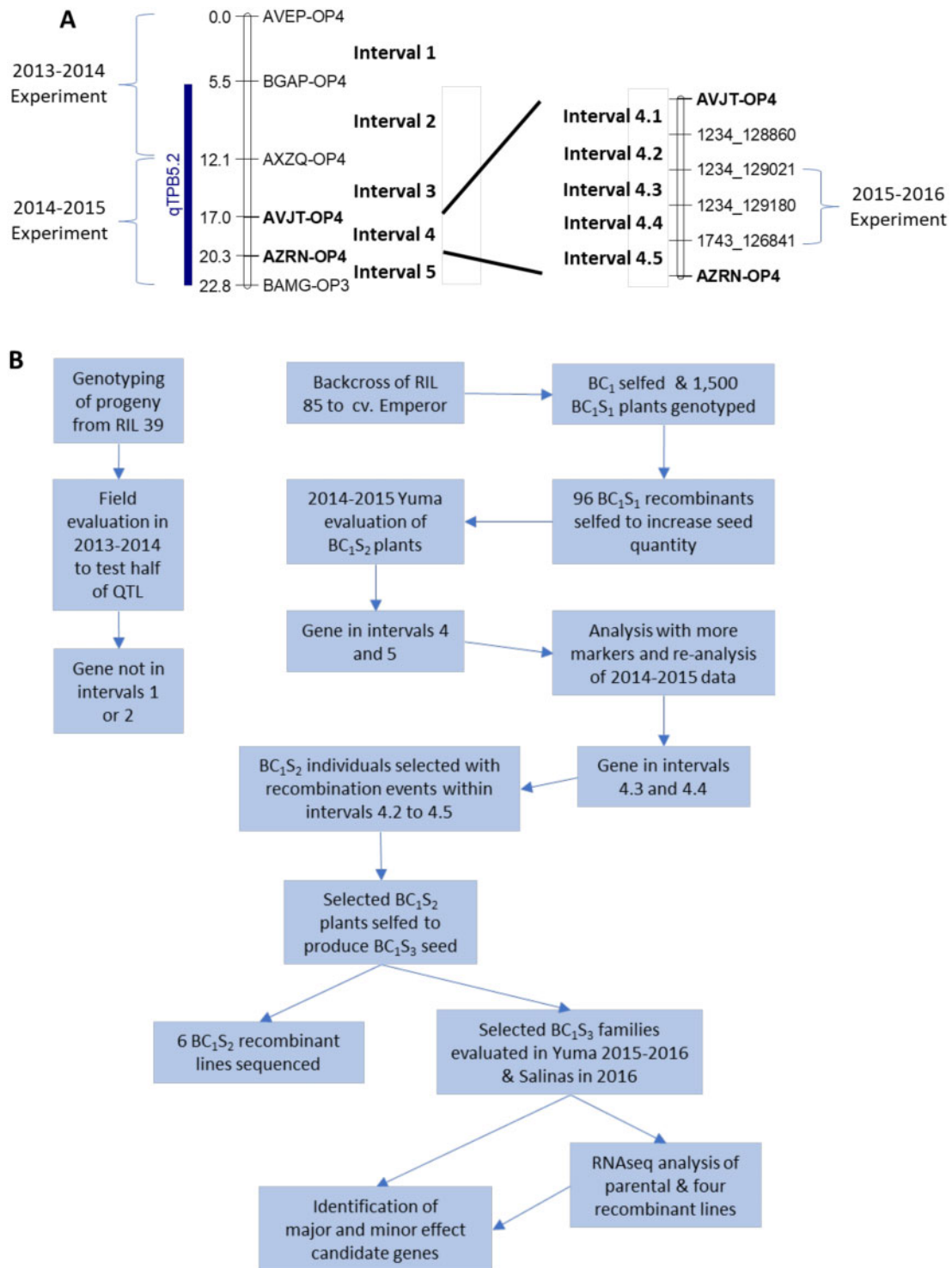


Figure 1 Summary of field experiments to identify candidate genes. (A) Representation of the investigated QTL region (numbers represent centimorgans estimated by Jenni et al. 2013) along with the magnified representation of interval 4, which was further divided to intervals 4.1–4.5. Marker names are labeled next to the whiskers and interval names are labeled between marker names. The prefix (EMPxELD) of markers EMPxELD_1234_128860, EMPxELD_1234_129021, EMPxELD_1234_129180, and EMPxELD_1743_126841 was removed. In Yuma, experiments were sown in winter 2013–2015 and evaluated in spring 2014–2016, respectively. In Salinas, one experiment was conducted in the spring of 2016. (B) Summary of the workflow.

Least-square means for tipburn incidence for each haplotype was estimated by using the emmeans (Lenth 2020) package. To back transform from the logit scale to the response scale, the regrid function in the emmeans package was used. Lower and upper highest posterior density (HPD) intervals (Chen and Shao

1999) were estimated using the confint function in the emmeans package.

Orthogonal contrasts were constructed using the contrast function in the emmeans package. The haplotypes to be compared was predetermined based on the goal of the experiment. If

the HPD interval did not include zero, then the difference in tipburn incidence was significant between the haplotypes. Analyses of leaf crinkliness at the margin of leaves, head firmness, plant weight, and tipburn severity were done using the lmer function in the lme4 package (Bates et al. 2015). Means and confidence intervals were constructed using the emmeans function from the emmeans package and orthogonal contrasts were constructed using the contrasts function. A significance level of $\alpha=0.05$ was used to declare significant differences.

Genotyping of RILs and recombinant individuals

To genotype recombinants, DNA was extracted from leaf tissue of plants at the three to four leaf stage using a custom protocol. Leaf tissue was ground frozen in liquid N₂ and thawed in 5 M guanidine isothiocyanate with 20 mM Tris-HCl (pH 6.75). PB buffer (Qiagen, Germantown, MD, USA) was used to clean up DNA in 96-well DNA binding plates (EconoSpin; Epoch Life Sciences, Sugar Land, TX, USA). The DNA was then washed with PE buffer (Qiagen) and 80% ethanol. The clean DNA was eluted in 10 mM Tris-HCl (pH 8.0).

The first set of primers (AVEP-OP4, BGAP-OP4, AXZQ-OP4, AVJT-OP4, AZRN-OP4, and BAMG-OP3) were designed based on available expressed sequence tags (<http://compgenomics.ucdavis.edu>; Stoffel et al. 2012). The second set of primers (EMPxELD_1234_128860, EMPxELD_1234_129021, EMPxELD_1234_129180, and EMPxELD_1743_126841) were designed by comparing sequence data between cvs. Emperor and El Dorado. The cvs. Emperor and El Dorado were sequenced to identify single nucleotide polymorphisms (SNPs) between them. Genomic DNA was extracted from 1 g of frozen leaf tissue of each of cvs. Emperor and El Dorado using a DNeasy Plant Maxi Kit (Qiagen). Libraries for sequencing were made using a Kapa Hyper Prep Kit (Kapa Biosystems, Wilmington, MA, USA) following the product specifications. DNA sequencing was conducted using 100 bp Illumina paired-end reads to 13× and 15× average genome coverage for cvs. Emperor and El Dorado, respectively. Sequence mapping and SNP calling against the lettuce reference cv. Salinas (Reyes-Chin-Wo et al. 2017) was done using the CLC Genomics Workbench (Qiagen). Read coverage within the QTL was used to identify potentially large indel polymorphisms. The software bedtools (Quinlan and Hall 2010) was run in the “genomecov-bga” mode to calculate nucleotide-level sequencing coverage to detect large deletions. Mapped reads within the QTL were visualized using the CLC Genomics Workbench v10 (Qiagen) to search for evidence of large insertions. PCR primers flanking SNPs of interest were designed to amplify polymorphic regions that were then analyzed for single strand conformation polymorphisms (Supplementary Table S4) in the RILs and their progeny.

Genomic sequence analysis of selected recombinants

Genomic DNA was extracted from 50 lettuce seeds of each of the seven recombinants using the DNeasy Plant Mini Kit (Qiagen). The DNA was run on a 2% agarose gel to check quality. Using a Covaris E220 sonicator (Covaris, Woburn, MA, USA), 1–3 μg DNA in 100 μl 1× TE buffer [10 mM Tris-HCl (pH 8), 0.1 mM EDTA] was sheared to 220 bp. Using a 1.5% agarose gel, the sheared DNA size was determined to be ~220 bp with most fragments no more than 500 bp. Agencourt AMPure XP beads (Beckman Coulter, Indianapolis, IN, USA) were diluted by adding 0.3 times the volume of a solution of 20% PEG (Mw: 4000 or 8000) and 2.5 M NaCl. The AMPure XP beads were used to clean up and concentrate

the fragmented DNA by adding 1.2:1 volumes of AMPure beads: sample.

Libraries for sequencing informative recombinants to further fine map candidate genes relative to cross-overs were prepared for sequencing using a custom protocol. End repair was done using the NEBNext End Repair Module with modifications. Instead of a 100 μl reaction, a 60 μl reaction was used with 1 to 3 μg of DNA in 51 μl, 6 μl of NEB 10× end repair buffer, and 3 μl of enzyme mix and incubating for 30 min at 20°C, then 15 min at 25°C. A clean up procedure was done by mixing with 80 μl of diluted AMPure XP beads as described above and eluting in 13 μl of elution buffer. A deoxyadenosine triphosphate (dATP) ligation was done in a 30 μl reaction by mixing 13 μl of eluted DNA, 15 μl of 2× T4 DNA ligase buffer (NEB, Cat. No. M0202S), 1 μl of dATP/NaCl solution (10 mM dATP; 300 mM NaCl), and 1 μl of Klenow (3′→5′ exonuclease; Enzymatics, Part No. P701-HC-L) and incubating for 30 min at 37°C, then 10 min at 75°C. Ligation of adapters was done by mixing 30 μl of the dATP ligation reaction with 5 μl of 10 μM premixed paired-end adapters, 4 μl of 2× ligation buffer, and 1 μl of T4 DNA ligase (Enzymatics, Cat. No. L603-HC-L). The 40 μl ligation reaction was incubated at 20°C for 10 min, 23°C for 10 min, 25°C for 10 min, and 70°C for 3 min. A final clean up step was done using undiluted AMPure beads following the manufacturer’s protocol.

DNA concentration was measured using a Qubit Fluorometer (Invitrogen) and Qubit dsDNA broad-range reagents (Thermo Fisher Scientific, Cat. No. Q32850). Individual libraries were pooled in equal concentrations and amplified by PCR in three reactions of 25 μl where 5–10 μl consisted of pooled library, 2.5 μl of 5 μM premixed paired-end PCR primers, 12.5 μl of Phusion 2× HF master mix (NEB, Ipswich, MA, USA), and 0–5 μl of DI water. PCR conditions were 98°C for 1 min followed by 14 cycles of 98°C for 10 s, 65°C for 30 s, and 72°C for 30 s then 72°C for 5 min. PCR reactions were then pooled and cleaned with 45 μl of undiluted AMPure beads and cleaning steps as described above. Libraries were sequenced using Illumina HiSeq4000 for 150 bp paired-end reads to 3× coverage.

The raw Illumina sequence data were processed by read quality trimming, alignment, and variant calling against the *L. sativa* reference genome (Reyes-Chin-Wo et al. 2017) using the CLC Genomics Workbench v10.1.1 (Qiagen). The quality of trimmed reads was checked using FastQC (Andrews 2010) to confirm high quality. Probabilistic variant detection was done using the CLC Genomics Workbench v10.1.1 (Qiagen) set to the following parameters: nonspecific matches were ignored, broken pairs were ignored, minimum coverage was set to 3, variant probability was set to 99.0, required variant count was set to 3, variant in nonspecific regions were ignored, presence in both forward and reverse reads was not required, and maximum expected variants were set to 2.

Sorted BAM files were created from the processed reads in CLC and used to produce an mpileup file with samtools (Li et al. 2009) using the v5 *L. sativa* reference genome (Reyes-Chin-Wo et al. 2017). The mpileup file was used to create a haplotype for every 10 Kb tiled across scaffolds Lsat_1_v5_g_5_1234 to Lsat_1_v5_g_5_1743 using custom Python scripts available at <https://github.com/alex-kozic/atgc-xyz>.

The wgsh_s2_GenotyperCleaner.py script with option 1 with default settings was used to remove SNPs with severely skewed genotype data (minor allele frequency < 10%), >80% of the samples missing, more than one sample displaying an indel in the alignment, or >10% of the samples genotyped as heterozygous. The wgsh_s3_SumByGroup.py script option “b” was used to group

SNPs every 10 Kb along the reference genome. The `wgsh_s4_GroupHaplotyper.py` script was used to convert groups of SNPs to haplotypes. The haplotype data were visualized by scaffold as ordered in v8 of the *L. sativa* reference genome assembly (Reyes-Chin-Wo et al. 2017) and additional SNPs were added in areas of interest by referring to the processed sequence in the CLC Genomics Workbench v10.1.1 (Qiagen) to identify positions of cross-overs in each recombinant line. The addition of SNPs through visual inspection with a few reads (>3) is valid because we are working with fixed lines (with one exception) and can confirm that the SNPs are real by referring to the sequence data of the parental lines, cvs. Emperor and El Dorado, which were sequenced at higher depth. In addition, the visual genotype call from processed sequence data can be corroborated by imputation.

RNA-seq analysis

A total of 30 samples for RNA-seq analysis were collected on March 31 from the YAC 2015–2016 field experiment from each of the five replicates of the six lines planted (Supplementary Table S5). Tissue was collected using a hole punch to make three ~2.5-cm deep cores from the bottom of three lettuce heads for each replicate, wrapped in aluminum foil, and quick frozen in liquid nitrogen. Due to the architecture of the iceberg lettuce head, this procedure sampled the edges of multiple leaves wrapped around the head; some necrotic leaf tissue symptomatic of tipburn was evident in the samples. The samples were transported to the lab on dry ice and stored at -80°C until further processing. Extraction of mRNA and random-primed, strand-specific libraries were prepared using the protocol from Zhong et al. (2011) with minor modifications. The 30 libraries were pooled and 150 bp paired-end sequencing was done using an Illumina HiSeq 4000 to a depth of ~30 million reads per sample.

Identical reads were removed using custom software. The processed reads were then quality trimmed using the `bbduk` algorithm in the `BBMap` package (Bushnell 2014). Trimmed reads were quality checked with `FastQC` (Andrews 2010).

Three analyses were performed with the RNA-seq data, two differential expression (DE) analyses and a k-mer analysis. For the two DE analyses, processed reads were aligned to the *L. sativa* reference genome (Reyes-Chin-Wo et al. 2017) using `STAR` software (Dobin et al. 2013). Read counts for each of the 67,975 annotated genes were extracted and the expression profiles across lines were analyzed using the `edgeR` package (Robinson et al. 2010; McCarthy et al. 2012). The data were normalized with the `TMM` algorithm prior to the DE analyses to adjust for between-sample differences in sequencing depth. For the first DE analysis, the expression profile of all other genotypes was compared against that of the resistant parent, cv. El Dorado. Significance for DE was established at an adjusted *P*-value < 0.05, which was generated by the `edgeR` package. For the second DE analysis, the expression of resistant lines was contrasted against that of all susceptible lines.

For the k-mer analysis, processed RNA-seq reads were bulked into two pools, one for all resistant lines and the other for all susceptible lines. Reads within each pool were broken into 31-bp sequences (31 mers or k-mers) and the frequency of all 31mers was counted using the software `Jellyfish` (Marçais and Kingsford 2011). k-mers with a frequency lower than six were discarded to reduce noise introduced by sequencing error. k-mers unique to each pool were then extracted and assembled into contigs using the software `ABYSS` (Jackman et al. 2017) with the parameters $k=25$, $c=0$, and $e=0$ (Fletcher et al. 2020). Contigs longer than

1 Kb were mapped against the lettuce reference assembly. Unmapped contigs were translated *in silico* using `ExpASy` (Gasteiger et al. 2003) and the function of the translated amino acid sequences were predicted using `NCBI BlastP` (Altschul et al. 1990).

Data availability

All raw data and Supplementary material are uploaded in figshare (maciasgonzalez.etal.TipburnRawData.xlsx and Gen_dissect_QTL_Tipburn_SuppMat_03_-02_21_submit.docx, respectively): <https://doi.org/10.25387/g3.14151611>. Raw genomic sequences of cv. Emperor, cv. El Dorado, and recombinants have been uploaded to the National Center for Biotechnology Information (PRJNA478460). RNA sequencing data have been submitted to GenBank (PRJNA557490).

Results

Yuma 2013–2014

The first trial in Yuma was conducted to test whether the genes determining tipburn are located in intervals 1 or 2. No significant differences in tipburn incidence were detected at the 95% confidence level between the 18 lines with contrasting haplotypes in intervals 1 and 2 (Table 1 and Figure 2). However, the cvs. El Dorado and Emperor had significant differences in tipburn incidence. These results for the control cvs. indicate that the environment was conducive to tipburn. Because no differences were seen between the experimental lines, we concluded that the genes determining tipburn resistance were not in intervals 1 and 2. Therefore, subsequent experiments focused on intervals 3–5.

Yuma 2014–2015

To test if the gene was in intervals 3–5, BC_1S_2 plants were selected with recombination events in these intervals and tested in the field at Yuma. Contrasts between haplotypes 3 and 4, 9 and 10, and 11 and 12 were significantly different at the 95% confidence level (Table 2 and Figure 3). This suggests that the determinant gene(s) are in intervals 4 or 5. Additional interstitial markers were designed in interval 4 and the lines with a recombination in interval 4 were genotyped with the new markers. The YAC 2014–2015 data for these lines were reanalyzed using the new marker data to test whether the location of the gene(s) was in intervals 4 or 5.

Four additional markers were then designed in interval 4 and were ordered based on v8 of the *L. sativa* reference genome assembly (Figure 1 and Supplementary Table S4). These additional four markers were used to position recombination events within this interval. The YAC 2014–2015 data were reanalyzed including the new marker data. There were significant differences between haplotypes 5.1 and 6.1, 11.1 and 12.1, and 11.2 and 12.2 at the 95% confidence level (Table 3 and Figure 4). This suggests that the determinant genes may be located between intervals 4.2 and 4.5.

Table 1 Contrast results of the Yuma 2013–2014 experiment

Contrast	Difference	LHPD	UHPD
El Dorado vs Emperor	−3.99	−5.92	−1.98
Haplotype 1 vs haplotype 2	0.27	−0.30	0.84

The difference in tipburn incidence is on a logit scale. The lower HPD (LHPD) and the upper HPD (UHPD) for intervals 1 and 2 bracketed zero; therefore, the difference in tipburn incidence between the experimental lines was not significant.

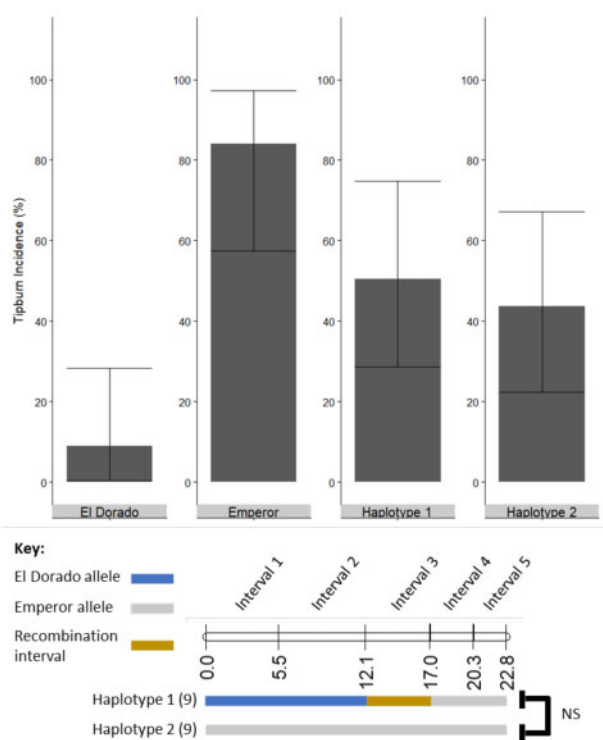


Figure 2 Tipburn incidence of each haplotype in the Yuma 2013–2014 field experiment. Haplotypes 1 and 2 are color coded to represent which segments of the QTL are homozygous for the cv. El Dorado allele or cv. Emperor allele. The number of lines tested with the same haplotype is reported in parenthesis. The comparisons made by orthogonal contrast at a significance level of $\alpha = 0.05$ are shown by haplotypes connected by brackets. Comparisons labeled “NS” were not significantly different. Comparisons labeled with an asterisk were significantly different. Error bars are the HPD intervals at the 95% confidence level.

Table 2 Results of the Yuma experiment in 2014–2015

Contrast	Difference	LHPD	UHPD
El Dorado vs Emperor	−1.05	−1.99	4.23
Haplotype 3 vs haplotype 4	−3.19	−4.56	−2.0
Haplotype 5 vs haplotype 6	−0.37	−1.46	0.66
Haplotype 7 vs haplotype 8	0.23	−0.70	1.25
Haplotype 9 vs haplotype 10	−4.65	−5.91	−3.46
Haplotype 11 vs haplotype 12	−1.77	−2.68	−0.78
Haplotype 13 vs haplotype 14	0.023	−0.92	1.37

The difference in tipburn incidence is in the logit scale. HPD intervals are estimated at the 95% confidence level. When the LHPD and the UHPD did not bracket zero, then the difference in tipburn incidence was significant.

Comparisons between haplotypes suggested that marker EMPxELD_1234_129180 (Figure 1) was highly correlated with tipburn incidence (Figure 4). Haplotype 11.3 had less tipburn than 12.3. Haplotype 11.3 is homozygous for the cv. El Dorado allele at marker EMPxELD_1234_129180, whereas haplotype 12.3 was heterozygous for the same marker. Similarly, the haplotype that is heterozygous at marker EMPxELD_1234_129180 did not have as much tipburn as haplotypes 17 and 18 (Figures 5 and 6), which were homozygous for the cv. Emperor allele at marker EMPxELD_1234_129180 but had slightly more tipburn than haplotypes 15 and 16, which were homozygous for the cv. El Dorado allele at marker EMPxELD_1234_129180.

Haplotypes of BC₁S₂ lines were examined to select lines for further testing. If marker EMPxELD_1234_129180 was tightly

linked to the determinant gene for tipburn expression, then there would be significant differences between contrasting haplotypes at marker EMPxELD_1234_129180 and no significant differences within haplotypes that are not contrasting at marker EMPxELD_1234_129180. A total of 10 lines were selected as potentially informative. Four of the selected recombinant lines with the cv. El Dorado allele at marker EMPxELD_1234_129180 (Figure 1) had flanking recombination events (i.e., recombination events in intervals 4.3 or 4.4). Six haplotypes had the cv. Emperor allele at marker EMPxELD_1234_129180 and had flanking recombination events but not in the same positions as the lines described above (i.e., recombination events in intervals 4.2 or 4.5). These lines were selected because no lines were found with the cv. Emperor allele at marker EMPxELD_1234_129180 and the same flanking recombination events as the other four lines. The nine selected BC₁S₂ haplotypes were selfed and BC₁S₃ was genotyped; 18 BC₁S₃ lines were selected for further evaluation in Yuma, Arizona and Salinas, California.

Yuma 2015–2016

These 18 homozygous BC₁S₃ lines were planted in YAC 2015–2016 to test whether there were significant differences in tipburn expression between lines that had contrasting alleles at marker EMPxELD_1234_129180 but no differences between lines that shared the resistant or susceptible EMPxELD_1234_129180 allele. There was significantly less tipburn incidence in haplotypes with the cv. El Dorado allele at marker EMPxELD_1234_129180 (e.g., haplotypes 15, 16, and 14G1227) compared with haplotypes with the cv. Emperor allele (e.g., haplotypes 17 and 18) at the 95% confidence level (Table 4 and Figure 5). This confirmed the tight association between the gene(s) for tipburn and marker EMPxELD_1234_129180. The haplotype 14G1227 had a much higher tipburn incidence than haplotypes 15 and 16 but no significant differences were detected at the 95% confidence level (Figure 5). However, the haplotype 14G1227 did have significantly more tipburn severity than haplotypes 15 and 16 (Supplementary Table S6; $P = 5.4e^{-03}$).

There were no significant differences in tipburn incidence between haplotypes 15 and 16 and between haplotypes 17 and 18 at the 95% confidence level (Table 4 and Figure 5). Tipburn incidence was less in cv. El Dorado than in cv. Emperor but not significant at the 95% confidence level (Table 4 and Figure 5).

Salinas 2016

The Yuma experiment was repeated the following summer in Salinas to evaluate the lines in a different environment. The Salinas 2016 experiment when evaluated 65 and 71 days after seed imbibition yielded similar results as the Yuma 2015–2016 experiment. There was a significant reduction in tipburn incidence between haplotypes 15, 16, and 14G1227 when compared with haplotypes 17 and 18 (Figure 6 and Table 5). There was no significant difference between haplotypes 15 and 16 compared with 14G1227 (Table 5). There was no significant difference between haplotypes 15 and 16 (Table 5). However, there was significantly more tipburn incidence in haplotype 17 than 18 at both harvest dates (Table 5 and Figure 6). Cv. El Dorado had significantly less tipburn incidence than cv. Emperor at 65 dai; however, at 75 dai cv. El Dorado did not have significantly less tipburn incidence than cv. Emperor at the 95% confidence level. Cv. El Dorado had the highest increase in tipburn incidence, going from ~5% to 60% at 71 dai (Figure 6). The recombinant lines did not have a difference in the rate of change for tipburn incidence. Haplotypes 15, 16, and 14G1227 did not show as dramatic an

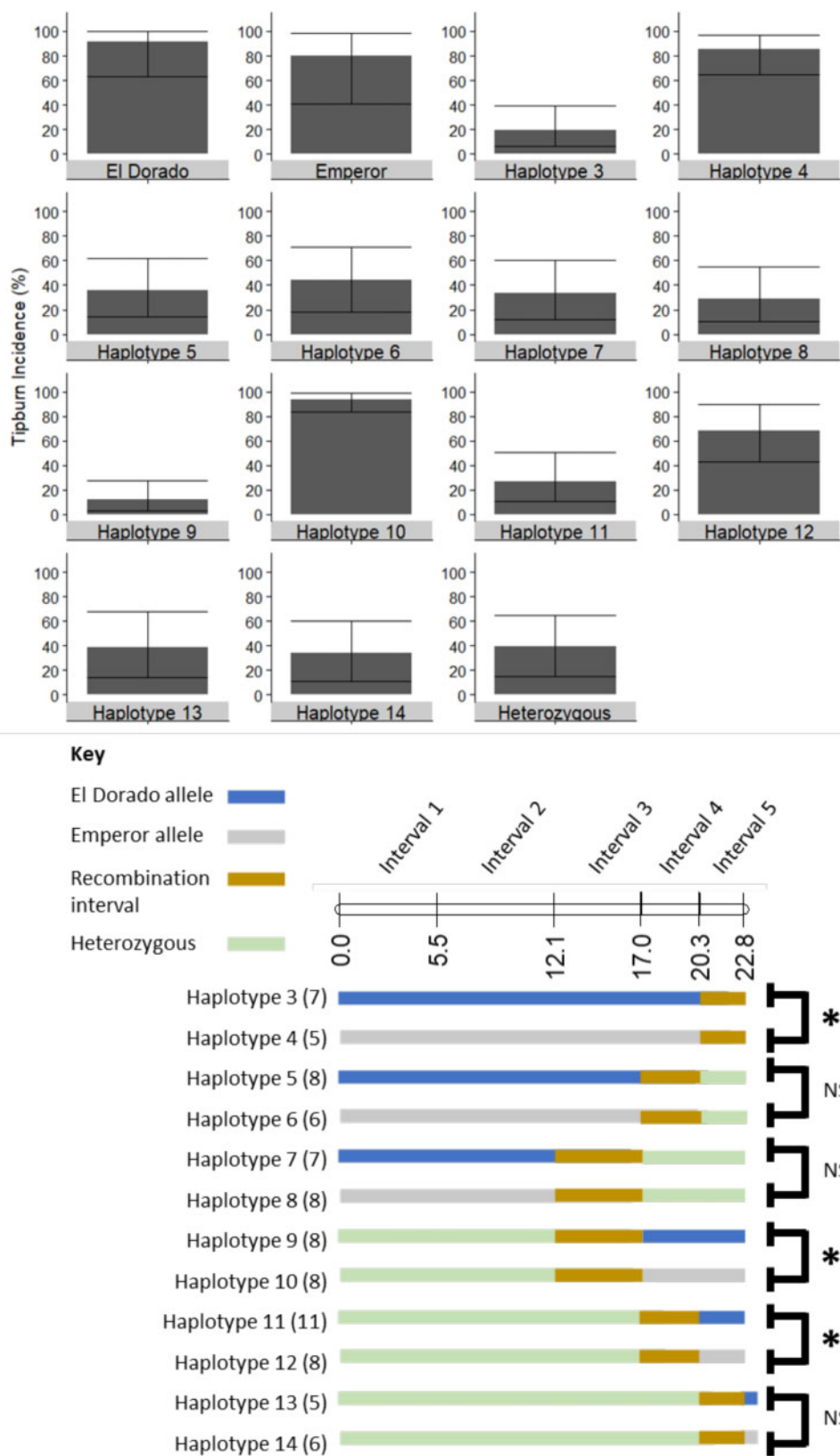


Figure 3 Tipburn incidence of each haplotype in the field experiment at Yuma in 2014–2015. Haplotypes 3–14 are color coded to represent segments of the QTL that are homozygous for the cv. El Dorado allele or cv. Emperor allele and those that are heterozygous. The number of lines tested with the same haplotype is reported in parenthesis. The comparisons made by orthogonal contrast at a significance level $\alpha = 0.05$ are shown by haplotypes connected by brackets. Comparisons labeled “NS” were not significantly different. Comparisons labeled with an asterisk were significantly different. Error bars are the HPD intervals at the 95% confidence level.

Table 3 Contrast results of the experiment at Yuma in 2014–2015 with the additional marker data

Contrast	Estimate	LHPD	UHPD
El Dorado vs Emperor	-1.20	-1.97	-4.25
Haplotype 5.1 vs haplotype 6.1	-2.47	-4.79	-0.19
Haplotype 5.2 vs haplotype 6.2	0.27	-1.79	2.3
Haplotype 5.3 vs haplotype 6.3	0.70	-1.20	2.53
Haplotype 11.1 vs haplotype 12.1	-3.40	-5.41	-1.44
Haplotype 11.2 vs haplotype 12.2	-3.29	-5.36	-1.14
Haplotype 11.3 vs haplotype 12.3	-0.82	-2.71	-0.90

Estimates are the difference in tipburn incidence in the logit scale. HPD intervals were estimated at 95% confidence level. When the LHPD and the UHPD did not bracket zero, then the difference in tipburn incidence was significant.

Table 4 Contrast results of the Yuma 2015–2016 experiment

Contrast	Estimate	LHPD	UHPD
El Dorado vs Emperor	-2.17	-6.19	2.16
Average of haplotypes 15, 16, and 14G1227 vs Average of Haplotype s17 and 18	-24.1	-36.1	-11.8
Average of haplotypes 15 and 16 vs 14G1227	-4.54	-11.45	1.93
Haplotype 15 vs haplotype 16	0.098	-3.18	3.06
Haplotype 17 vs haplotype 18	0.99	-1.86	3.71

Estimates are the difference in tipburn incidence in the logit scale. HPD intervals were estimated at the 95% confidence level. When the LHPD and the UHPD did not bracket zero, then the difference in tipburn incidence was significant.

increase in tipburn as cv. El Dorado. Therefore, the data from Yuma and Salinas indicated that there was a gene between markers EMPxELD_1234_129021 and EMPxELD_1743_126841 (i.e., intervals 4.3 and 4.4) that can reduce tipburn incidence by 60% (Figures 5 and 6).

The comparisons between haplotypes 17 and 18 provided additional information indicative of a second gene influencing tipburn outside of the intervals 4.3 and 4.4. Haplotype 17 had significantly more tipburn incidence than haplotype 18 (Figure 6 and Table 5). Similarly, haplotype 15 showed more tipburn incidence than haplotype 16 (Figure 6). This is consistent with a second gene located between AVEP-OP4 and EMPxELD_1234_129021 of lesser effect contributing to the tipburn phenotype, for which the cv. Emperor allele confers resistance rather than the cv. El Dorado allele.

Genomic sequence analysis

The above marker analysis narrowed the position of the major gene(s) for tipburn to three scaffolds spanning ~1294 Kb, which contained 23 annotated genes in the reference genome assembly (Reyes-Chin-Wo et al. 2017). To further fine map the location of genes for tipburn resistance, the six tipburn resistant BC₁S₂ recombinants with cross-overs between EMPxELD_1234_129021 and EMPxELD_1743_126841 were sequenced. Haplotypes were determined for 10 Kb intervals across the EMPxELD_1234_129021 to EMPxELD_1743_126841 region and individual SNPs were determined across the candidate region (Figure 7). This analysis revealed the relative positions of recombination events in the v8 reference genome relative to genes in the region. Lines 15G206 and 15G209 had a recombination event at position ~253,299,305 within scaffold Lsat_1_v5_g_5_1234. The heterozygous haplotype

14G1227 had a recombination event in scaffold Lsat_1_v5_g_5_1234 at position ~253,276,149. Haplotypes 15G368, 15G369, and 15G370 had a recombination event at position ~252,012,564 within scaffold Lsat_1_v5_g_5_1743. Haplotype 15G277 had a recombination event at position ~252,470,667 of scaffold Lsat_1_v5_g_5_517. Therefore, the gene(s) for tipburn resistance are between position 253,304,091 of scaffold Lsat_1_v5_g_5_1234 and position 252,200,668 of scaffold Lsat_1_v5_g_5_517. This analysis reduced the candidate region to 877 Kb according to Gbrowse v9 of the *L. sativa* cv. Salinas genome, which contained 12 genes.

There were very few sequence polymorphisms between cvs. Emperor and El Dorado in these 12 genes (Supplementary Table S7). Only three of the 12 genes had SNPs. Lsat_1_v5_gn_5_129180 was the only gene with a SNP in an exon, which was the marker EMPxELD_1234_129180 used in the above analyses. Lsat_1_v5_gn_5_127001 and Lsat_1_v5_gn_5_127161 had SNPs in introns. The ~5.4 Kb insertion was evident in the 3'UTR region of the primary transcript of Lsat_1_v5_gn_5_127021, which had been reported previously (Seki et al. 2020). No additional large deletions were detectable with certainty given the variation in sequencing depth of cv. Emperor. Six of these 12 genes had mutations in the 5 Kb upstream of the coding region and therefore had potential promoter polymorphisms, including Lsat_1_v5_gn_5_129040, Lsat_1_v5_gn_5_129201, Lsat_1_v5_gn_5_126960, Lsat_1_v5_gn_5_127021, Lsat_1_v5_gn_5_127080, and Lsat_1_v5_gn_5_127161 (Supplementary Table S7).

RNA-seq analysis

To assist in the identification of candidate genes, inner leaves of cvs. Emperor and El Dorado and four BC₁S₃ recombinant lines, two resistant and two susceptible, were analyzed by RNA-seq (Supplementary Table S5). Expression was not detected for 7 of the 12 genes in the 877 Kb region.

Three independent DE analyses were performed. First, we compared the expression between the resistant parent, El Dorado, and each other line. Only two genes, Lsat_1_v5_gn_5_129241 and Lsat_1_v5_gn_5_127021, were significantly DE between all susceptible lines and the resistant cv. El Dorado (Table 6). Lsat_1_v5_gn_129241 encodes a superoxide dismutase, and Lsat_1_v5_gn_127021 encodes a Teosinte branched1/Cycloidea/Proliferating Cell factor 4 (TCP4) transcription factor-like protein. Expression of genes Lsat_1_v5_gn_5_129040 and Lsat_1_v5_gn_5_129180, which are annotated as a vacuolar proton-Ca²⁺ exchanger protein, was only DE between the susceptible progeny 15G267 and the resistant parent, El Dorado, but not between any other susceptible lines and El Dorado.

Second, we formed two pools of RNA-seq results, one pool for all resistant lines (El Dorado, 15G209, and 15G368) and the other for all susceptible lines (Emperor, 15G174, and 15G267) and performed DE analysis between the two pools. All five expressed genes within the QTL were identified as DE genes with an adjusted P-value < 0.05 (Table 7).

Third, we performed k-mer analysis for the two pools of RNA-seq results. k-mers unique to the susceptible pool assembled into 83 large (>1 Kb) contigs, whereas k-mers unique to the resistant pool assembled into 37 large contigs. Interestingly, the cDNA sequence of Lsat_1_v5_gn_5_129180 was found among the large contigs unique to the susceptible pool. Most of the rest of the pool-specific contigs mapped to outside of the tipburn QTLs in the reference genome. Seventeen of the pool-specific contigs did

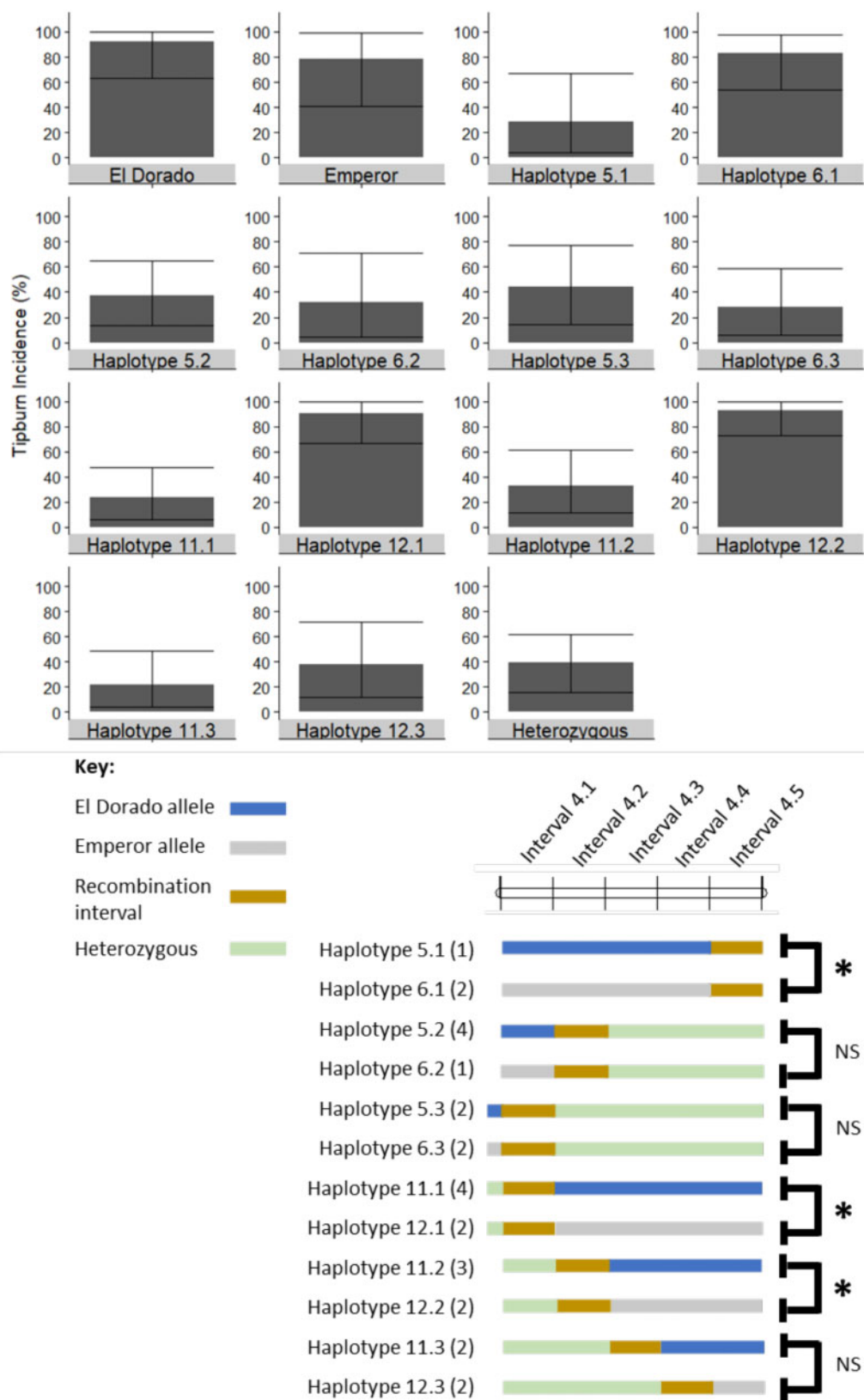


Figure 4 Tipburn incidence of the haplotypes in the Yuma 2014–2015 experiment with new marker data designed to dissect interval 4. Haplotypes are color coded to represent the segments of interval 4 that are homozygous for cv. El Dorado allele or cv. Emperador allele and heterozygous regions. The number of lines tested with the same haplotype is reported in parenthesis. The comparisons made by orthogonal contrast at $\alpha = 0.05$ significance level are shown by haplotypes connected by brackets. Comparisons labeled “NS” were not significantly different. Comparisons labeled with an asterisk were significantly different. Error bars are the HPD intervals at the 95% confidence level.

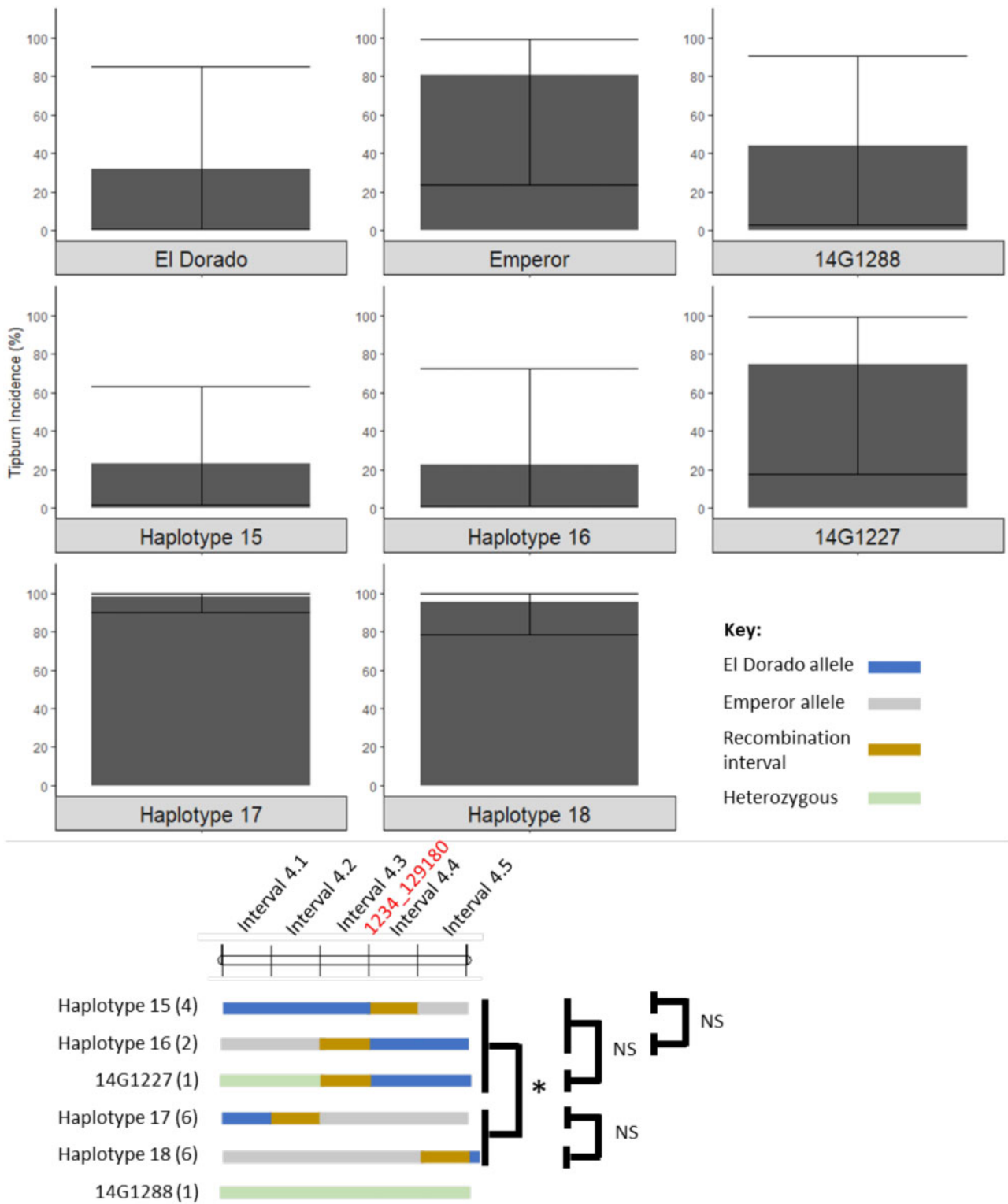


Figure 5 Tipburn incidence of the haplotypes in the Yuma 2015–2016 experiment. Haplotypes are color coded to represent the segments of interval 4 that are homozygous for cv. El Dorado allele or cv. Emperor allele and heterozygous regions. The number of lines tested with the same haplotype is reported in parenthesis. The comparisons made by orthogonal contrast at a significance level of $\alpha = 0.05$ are shown by haplotypes connected by brackets. Comparisons labeled “NS” were not significantly different. Comparisons labeled with an asterisk were significantly different. Error bars are the HPD intervals at the 95% confidence level.

not map to the lettuce reference genome and instead encoded fungal or viral proteins.

The minor QTL is flanked by AVEP-OP4 and Lsat_1_v5_gn_5_129040. A similar RNA-seq analysis was

conducted for this region to identify DE genes. The cv. El Dorado allele is the susceptible allele in the minor QTL region. The RNA-seq results compared a pool of lines with the susceptible allele (15G368, 15G174, and cv. El Dorado) to a pool of lines with the

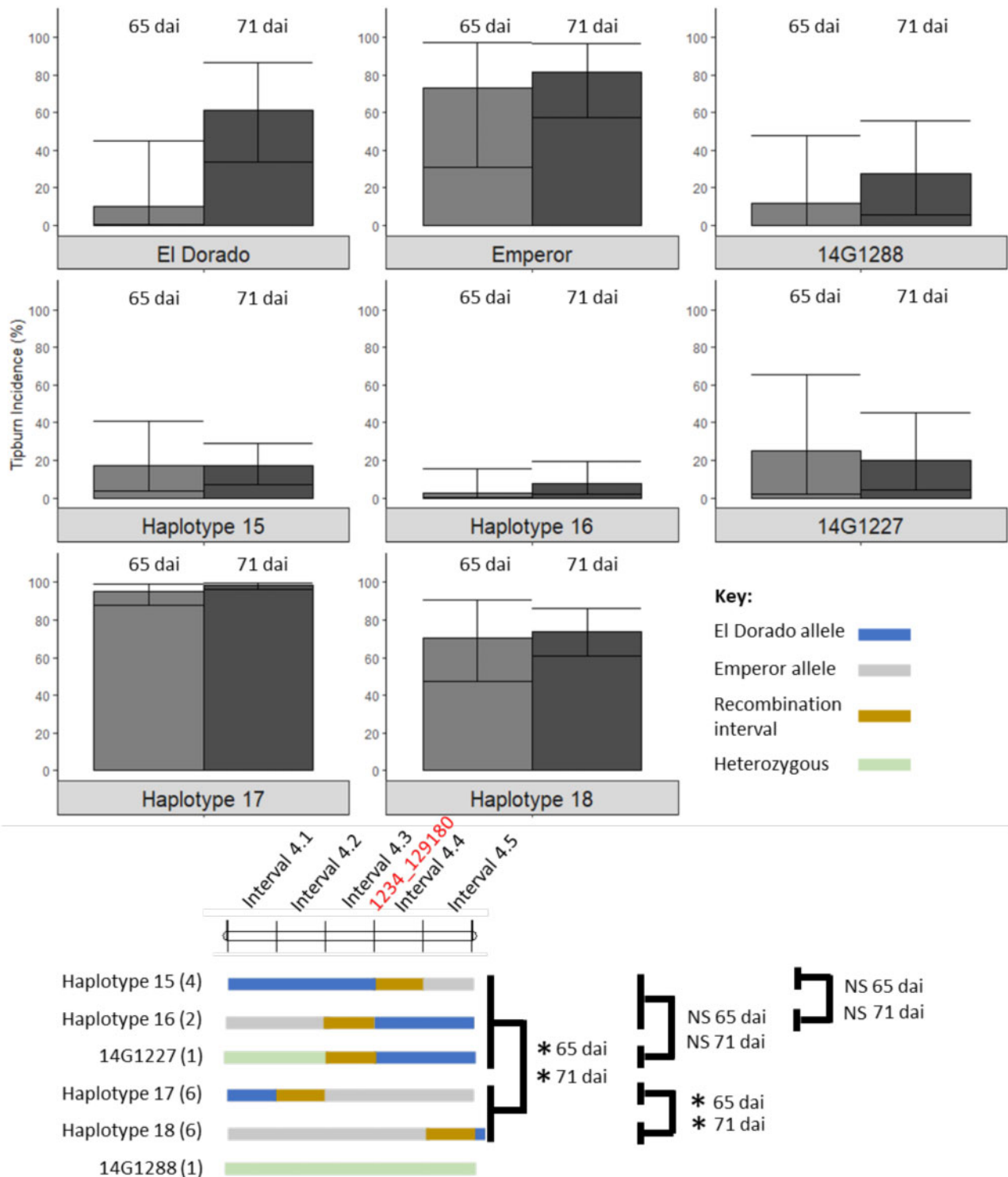


Figure 6 Tipburn incidence of the haplotypes in the Salinas 2016 field experiment. The haplotypes were evaluated twice, once at 65 and 71 dai. Haplotypes are color coded to represent the segments of interval 4 that are homozygous for cv. El Dorado allele or cv. Emperor allele and heterozygous regions. The number of lines tested with the same haplotype is reported in parentheses. The comparisons made by orthogonal contrast at a significance level of $\alpha = 0.05$ are shown by haplotypes connected by brackets. Comparisons labeled “NS” were not significantly different. Comparisons labeled with an asterisk were significantly different. Error bars are the HPD intervals at the 95% confidence level.

resistant allele (15G209, 15G267, and cv. Emperor). There are ~435 genes in this interval, of which 39 were DE between the two pools (Supplementary Table S8). These genes encoded for a wide range of activities involved in growth, metabolism, and ion transport. Interestingly, *Lsat_1_v5_gn_5_140040* is in a 27.5 Kb region where no reads from cv. Emperor mapped to the reference

genome and is potentially an indel; therefore, *Lsat_1_v5_gn_5_140040* may be missing from cv. Emperor.

Other traits

The results for tipburn severity were very similar to the results of tipburn incidence (Supplementary Table S6); therefore, these are

not discussed further. There was significantly more leaf crinkliness in haplotypes with the cv. Emperor allele at intervals 4.3 and 4.4 in both Yuma, Arizona and Salinas, California ($P < 1.0e^{-04}$; Supplementary Table S9). There were no significant differences in leaf crinkliness between haplotypes 15 and 16 in either Yuma or Salinas ($P = 0.15$ and 1.0 , respectively). However, haplotype 17 had significantly more leaf crinkliness in the Salinas experiment ($P = 5.4e^{-03}$). This is because occasionally some of the lines with haplotype 18 were scored as having less leaf crinkliness. cv.

Table 5 Results of the Salinas 2016 experiment 65 and 71 dai

Contrast	65 dai			71 dai		
	Estimate	LHPD	UHPD	Estimate	LHPD	UHPD
El Dorado vs Emperor	-3.17	-6.19	-0.14	-1.08	-2.82	0.80
Average of haplotypes 15, 16, and 14G1227 vs average of haplotypes 17 and 18	-24.4	-32.0	-15.9	-26.7	-32.3	-21.4
Average of haplotypes 15 and 16 vs 14G1227	-3.01	-7.74	1.21	-1.21	-4.39	1.67
Haplotype 15 vs haplotype 16	2.07	-0.34	4.59	0.88	-0.43	2.42
Haplotype 17 vs haplotype 18	2.10	0.68	3.66	3.13	1.92	4.46

Estimates are the difference in tipburn incidence in the logit scale. HPD intervals were estimated at the 95% confidence level. When the LHPD and the UHPD did not bracket zero, then the difference in tipburn incidence was significant.

Emperor has the crinklier leaf phenotype and the susceptibility allele at the major tipburn QTL. Therefore, genes controlling leaf morphology could be in this same region or may have a pleiotropic effect on tipburn incidence.

There was no significant difference in firmness between cvs. Emperor and El Dorado but haplotypes 17 and 18 had significantly more firmness compared with haplotypes 15, 16, and 14G1227 in all locations and time points (Supplementary Table S9). Haplotype 15 had significantly more firmness than haplotype 16 in the Salinas experiment at both timepoints ($P = 6.8e^{-03}$ and 0.026). There were no significant differences in head firmness between haplotypes 17 and 18. Firmness is a proxy for maturity, growth rate, and head architecture; the firmer lines were more prone to tipburn. Therefore, genes controlling growth rate and/or head architecture may be influencing tipburn incidence.

There was significantly greater fresh plant weight in haplotypes 15, 16, and 14G1227 compared with haplotypes 17 and 18 in the Yuma experiment, but in Salinas at 65 dai, the group with the cv. El Dorado allele had significantly less plant weight ($P < 1.0e^{-04}$ and $P = 4.2e^{-03}$, respectively; Supplementary Table S9). On average, haplotypes 15, 16, and 14G1227 yielded 455 g more than haplotypes 17 and 18. In Salinas, haplotypes 15, 16, and 14G1227 yielded 65 g less than haplotypes 17 and 18. There was no significant difference within the cv. El Dorado haplotypes but there was a significant difference within the cv. Emperor haplotypes in Yuma ($P = 7.1e^{-03}$). Therefore, there was an uncoupling between tipburn and plant fresh weight in the Yuma environment. QTLs have been identified for plant fresh weight elsewhere in the genome (Macias-González et al. 2019, 2020); therefore, tipburn is not obligatorily driven by plant weight.

Table 6 RNA-seq analysis results for genes located within the ~877 Kb candidate region

Tipburn incidence	15G209		15G368		15G174		15G267		Emperor	
	82.60%	82.60%	82.60%	82.60%	82.60%	82.60%	82.60%	82.60%	82.60%	82.60%
Gene										
Lsat_1_v5_g-n_5_129040	NS	-	NS	D	NS	E	4.43	E	NS	E
Lsat_1_v5_g-n_5_129100	ne	D	ne	D	ne	E	ne	E	ne	E
Lsat_1_v5_g-n_5_129180	NS	D	NS	D	NS	E	0.70	E	NS	E
Lsat_1_v5_g-n_5_129201	NS	D	NS	D	NS	E	-0.45	E	NS	E
Lsat_1_v5_g-n_5_129241	NS	D	NS	D	0.71	E	-0.97	E	0.78	E
Lsat_1_v5_g-n_5_126960	ne	D	ne	D	ne	E	ne	E	ne	E
Lsat_1_v5_g-n_5_127001	ne	D	ne	D	ne	E	ne	E	ne	E
Lsat_1_v5_g-n_5_127021	NS	D	NS	D	-0.49	E	0.65	E	-0.54	E
Lsat_1_v5_g-n_5_127080	ne	D	ne	D	ne	E	ne	E	ne	E
Lsat_1_v5_g-n_5_127101	ne	D	ne	D	ne	E	ne	E	ne	E
Lsat_1_v5_g-n_5_127121	ne	D	ne	D	ne	E	ne	E	ne	E
Lsat_1_v5_g-n_5_127161	ne	D	ne	D	ne	E	ne	E	ne	E

The expression profile of cv. El Dorado was used as the reference. If the genes were differentially expressed, the \log_2 fold change in comparison with cv. El Dorado is provided. NS = gene was expressed but not differentially expressed. ne = no expression detected. D = cv. El Dorado allele. E = cv. Emperor allele.

V5 Scaffold	V8 Start Position	V8 End Position	Number Of SNPs	Number Of							Marker	Visual Inspection	Interval
				14G1227	15G206	15G209	15G277	15G368	15G369	15G370			
Lsat_1_v5_g_5_1743	251,732,565	251,742,564	75	D	D	D	E	E	E	E			Interval 4.5
Lsat_1_v5_g_5_1743	251,802,565	251,812,564	3	D	D	D	E	E	E	E			
Lsat_1_v5_g_5_1743	251,832,565	251,842,564	1	D	D	D	E	E	E	E			
Lsat_1_v5_g_5_1743	251,842,565	251,852,564	2	D	D	D	E	E	E	E			
Lsat_1_v5_g_5_1743	251,852,565	251,862,564	2	D	D	D	E	E	E	E			
Lsat_1_v5_g_5_1743	251,862,565	251,872,564	1	D	D	D	E	E	E	E			
Lsat_1_v5_g_5_1743	251,892,565	251,902,564	2	D	D	D	E	E	E	E			
Lsat_1_v5_g_5_1743	251,902,565	251,912,564	3	D	D	D	E	E	E	E			
Lsat_1_v5_g_5_1743	251,912,565	251,922,564	1	D	D	D	E	E	E	E			
Lsat_1_v5_g_5_1743	251,922,565	251,932,564	1	D	D	D	E	E	E	E			
Lsat_1_v5_g_5_1743	251,932,565	251,942,564	2	D	D	D	E	E	E	E			
Lsat_1_v5_g_5_1743	251,942,565	251,952,564	4	D	D	D	E	E	E	E			
Lsat_1_v5_g_5_1743	251,952,565	251,962,564	3	D	D	D	E	E	E	E			
Lsat_1_v5_g_5_1743	251,962,565	251,972,564	1	D	D	D	E	E	E	E			
Lsat_1_v5_g_5_1743	251,972,565	251,982,564	1	D	D	D	E	E	E	E			
Lsat_1_v5_g_5_1743	252,002,565	252,012,564	5	D	D	D	E	E	E	E	EMPxELD_1743_126841		
Lsat_1_v5_g_5_1743	252,032,565	252,042,564	2	D	D	D	E	D	D	D			
Lsat_1_v5_g_5_1743	252,052,565	252,062,564	1	D	D	D	E	D	D	D			
Lsat_1_v5_g_5_1743	252,062,565	252,072,564	1	D	D	D	E	D	D	D			
Lsat_1_v5_g_5_1743	252,082,565	252,092,564	1	D	D	D	E	D	D	D			
Lsat_1_v5_g_5_1743	252,092,565	252,102,564	1	D	D	D	E	D	D	D			
Lsat_1_v5_g_5_1743	252,102,565	252,112,564	1	D	D	D	E	D	D	D			
Lsat_1_v5_g_5_1743	252,112,565	252,122,564	1	D	D	D	E	D	D	D			
Lsat_1_v5_g_5_1743	252,122,565	252,132,564	2	D	D	D	E	D	D	D			
Lsat_1_v5_g_5_1743	252,132,565	252,141,217	1	-	D	D	E	D	D	D			
Lsat_1_v5_g_5_517	252,170,025	252,170,667	1	D	D	D	E	D	D	D			
Lsat_1_v5_g_5_517	252,190,668	252,200,667	1	D	D	D	E	D	D	D			
Lsat_1_v5_g_5_517	252,200,668	252,210,667	2	D	D	D	F	D	D	D			
Lsat_1_v5_g_5_517	252,480,668	252,470,667	1	D	D	D	D	D	D	D			
Lsat_1_v5_g_5_517	252,515,074	252,519,790	2	D	D	D	D	D	D	-		X	
Lsat_1_v5_g_5_517	252,739,268	252,739,868	2	D	D	D	D	D	D	D		X	
Lsat_1_v5_g_5_1234	253,155,473	253,155,670	2	D	D	D	D	D	D	D			
Lsat_1_v5_g_5_1234	253,201,549	253,201,549	1	D	D	D	D	D	D	D	EMPxELD_1234_129180		
Lsat_1_v5_g_5_1234	253,230,666	253,230,666	1	D	D	D	D	D	D	D		X	
Lsat_1_v5_g_5_1234	253,231,153	253,231,153	1	D	D	D	D	D	D	D		X	
Lsat_1_v5_g_5_1234	253,247,178	253,247,178	1	D	D	D	D	D	D	D		X	
Lsat_1_v5_g_5_1234	253,263,347	253,263,347	1	D	D	D	D	D	D	D		X	
Lsat_1_v5_g_5_1234	253,273,128	253,276,149	1	H	D	D	D	D	D	D			
Lsat_1_v5_g_5_1234	253,299,305	253,299,305	1	H	D	D	D	D	D	D		X	
Lsat_1_v5_g_5_1234	253,304,091	253,304,091	1	H	E	E	D	D	D	D	EMPxELD_1234_129021		
Lsat_1_v5_g_5_1234	253,306,150	253,316,149	2	H	E	E	D	D	D	D			
Lsat_1_v5_g_5_1234	253,346,150	253,356,149	8	H	E	E	D	D	D	D			
Lsat_1_v5_g_5_1234	253,356,150	253,366,149	6	H	E	E	D	D	D	D			
Lsat_1_v5_g_5_1234	253,366,150	253,376,149	33	H	E	E	D	D	D	D			
Lsat_1_v5_g_5_1234	253,376,150	253,386,149	5	H	E	E	D	D	D	D			
Lsat_1_v5_g_5_1234	253,386,150	253,396,149	27	H	E	E	D	D	D	D			
Lsat_1_v5_g_5_1234	253,396,150	253,406,149	16	H	E	E	D	D	D	D			
Lsat_1_v5_g_5_1234	253,406,150	253,416,149	23	H	E	E	D	D	D	D			
Lsat_1_v5_g_5_1234	253,416,150	253,426,149	49	H	E	E	D	D	D	D			
Lsat_1_v5_g_5_1234	253,426,150	253,436,149	51	H	E	E	D	D	D	D			
Lsat_1_v5_g_5_1234	253,436,150	253,446,149	11	H	E	E	D	D	D	D			
Lsat_1_v5_g_5_1234	253,446,150	253,456,149	15	H	E	E	D	D	D	D			
Lsat_1_v5_g_5_1234	253,456,150	253,466,149	27	H	E	E	D	D	D	D			
Lsat_1_v5_g_5_1234	253,486,150	253,496,149	9	H	E	E	D	D	D	D	EMPxELD_1234_18860		

Figure 7 Genomic DNA sequence results of informative recombinants further fine map the location of candidate genes to the box outlined in bold. Haplotyping was done for every 10 Kb and some genotyping was added by visual inspection of the raw sequence or by available markers. Genotypes called by markers are reported under the “Marker” column by the marker name. Genotypes called by visual inspection of the raw sequence are reported under the column “Visual Inspection” with an “X.” The start and end positions are reported as given in version 5 of the lettuce genome (Reyes-Chin-wo et al. 2017). Note that the orientation of Lsat_1_v5_g_5_1743 is inverted. The resistant allele (D) is from cv. El Dorado, the susceptible allele (E) is from cv. Emperor, and the heterozygous genotype is denoted by H.

Table 7 Pooled RNA-seq analysis results for differentially expressed genes located within the ~877 Kb candidate region

Gene	Log2 fold change	Adjusted P-value
Lsat_1_v5_gn_5_129040	-0.50	0.0051
Lsat_1_v5_gn_5_129180	-2.9	0.011
Lsat_1_v5_gn_5_129201	0.33	0.005
Lsat_1_v5_gn_5_129241	-0.52	8.4e ⁻⁰⁶
Lsat_1_v5_gn_5_127021	0.64	1.7e ⁻⁰⁵

Comparison was done between a pool of lines with the susceptible allele (15G174, 15G267, and cv. Emperor) against a pool of lines with the resistant allele (15G209, 15G368, and cv. El Dorado).

Discussion

In this study, we genetically dissected the major QTL previously identified using multiple RIL populations (Macias-González et al. 2019) and identified candidate genes for resistance to tipburn.

The QTL was dissected in two stages using RILs derived from cvs. Emperor × El Dorado (Jenni et al. 2013). First, half of the QTL region was tested for presence of tipburn genes by comparing lines with contrasting haplotypes in the target region for differences in tipburn incidence. Since no differences were detected in one half of the QTL region, new lines were developed with recombination events in the other half of the QTL region. This required large-scale field experiments to evaluate tipburn phenotypes on a line rather than an individual plant basis. The combined field phenotyping and genotyping analyses revealed a genomic region of 877 Kb encoding 12 genes that was significantly associated with tipburn incidence. In addition, these experiments provided evidence for a second gene of minor effect outside of the 877 Kb region but within the overall region of qTPB5.2.

Two of the 12 genes identified in the major-effect interval associated with tipburn, Lsat_1_v5_gn_5_129040 and Lsat_1_v5_gn_5_129180, encode proteins with sequence similarity to calcium transporters. These genes were differentially

expressed between pools of lines with the resistant allele (15G209, 15G368, and cv. El Dorado) and lines with the susceptible allele (15G174, 15G267, and cv. Emperor) on the major QTL. k-mers unique to the susceptible transcriptome pool assembled into the transcript of *Lsat_1_v5_gn_5_129180*, consistent with this gene functioning in tipburn susceptibility. These genes are good candidates because their function is congruent with the association of tipburn with local calcium deficiency. The *Arabidopsis thaliana* ortholog At1g53210, expressed in leaf and shoot tissue, is localized in the plasma membrane and plays a role in Ca^{2+} homeostasis during salt and heat stress (Wang et al. 2012), auxin signaling, and flowering time (Li et al. 2016). *Lsat_1_v5_gn_5_129180* had a missense alanine to valine polymorphism in the exon; this was not located in the Na^+/Ca^+ exchanger or EF-hand-like domains. The EF-hand-like domain is thought to deregulate the $\text{Na}^+/\text{Ca}^{2+}$ exchanger activity based on enhanced activity of the transporter when the EF-hand motifs were deleted (Li et al. 2016). If this mutation is responsible for the differences in tipburn incidence, then it could be due to a change in protein folding. Alanine and valine have similar chemical properties; they are both small, nonpolar, and hydrophobic (Livingstone and Barton 1993). However, valine is more hydrophobic than alanine and has a greater preference to be within hydrophobic cores (Betts and Russell 2003). An alanine to valine substitution or *vice versa* has been shown to cause significant changes in function, expression, and physical conformation of proteins (Gradstein et al. 2016; Johnson et al. 2016; Cantu et al. 2017). Expression of *Lsat_1_v5_gn_5_129180* has been reported previously (De Cremer et al. 2013); however, expression and differences in expression were not detected in the tissue collected in this study, even though some collected tissue showed symptoms of tipburn. Future experiments should analyze leaf tissue at different, earlier stages of maturation. At1g53210 is expressed from the 2- to 12-leaf stages in *Arabidopsis*; expression may be similar in lettuce. Transgenics expressing the *Lsat_1_v5_gn_5_129180* promoter fused to a reporter gene might be informative.

Lsat_1_v5_gn_5_127021 and *Lsat_1_v5_gn_5_127080* are both genes encoding TCP4 and TCP10 transcription factors (Supplementary Table S7) belonging to the class II CIN-TCP transcription factors. They can be responsible for the differences in leaf crinkliness because homologs in *Arabidopsis* have a similar role. In *Arabidopsis*, these transcription factors interact with phytohormone pathways (Sarvepalli and Nath 2011a; Nicolas and Cubas 2016), regulate petal (Nag et al. 2009) and leaf growth mediated by cell proliferation (Palatnik et al. 2003; Efroni et al. 2008; Rodriguez et al. 2010; Sarvepalli and Nath 2011b; Schommer et al. 2014), and are negatively regulated by micro-RNA *miR319a* (Nicolas and Cubas 2016). Down regulation of class II TCP transcription factors by *miR319a* or knockouts of TCP factors have resulted in a characteristic crinkly leaf phenotype in both *Arabidopsis* and *Antirrhinum major* (Nath et al. 2003; Palatnik et al. 2003; Koyama et al. 2007, 2010; Efroni et al. 2008). There is a gene dosage effect between leaf crinkliness and the number of CIN-TCP genes knocked out (Koyama et al. 2010).

In this study, the TCP 4 ortholog was down regulated in cv. Emperor and 15G174 but not 15G267 (all susceptible lines) when compared with cv. El Dorado (Table 6). Cv. Emperor, 15G174, and 15G267 all showed the crinkly leaf phenotype. However, in the pooled analysis, the results showed that this gene was upregulated (Table 7). It is unclear why there is this discrepancy, but it is possible that the expression of the gene changes over time. The results indicate that this gene is differentially expressed between resistant and susceptible pools, which is consistent with the

findings reported in Seki et al. (2020) who attributed the differential gene expression to a retrotransposon insertion in the 3'-UTR region of the gene in Emperor type cvs., such as cv. Emperor, and found a strong correlation to higher leaf crinkliness and late bolting in this gene. If this gene has a pleiotropic effect on tipburn, it could be due to the effects that this gene has on cell proliferation. The susceptible allele would result in greater cell proliferation in the Emperor type than in the El Dorado type, resulting in a higher demand for calcium in the proliferating cells. Given that calcium transport to tissues is mainly determined by the transpiration stream and that leaves growing under high humidity (such as the internal leaves of iceberg lettuce) would receive less calcium (Barta and Tibbitts 1986), we propose the following hypothesis: (1) greater cell proliferation due to downregulation of CIN-TCP causes higher demand for calcium; (2) reduced transpiration from younger leaves inside the head results in a reduced supply of calcium to proliferating cells; and (3) a shortage of calcium supply to proliferating cells in these younger leaves results in tipburn. Future studies should knockout or interfere with the gene expression of the genes in this 877 Kb region to identify which gene knockout or knockdown results in higher tipburn incidence or severity. Finding this correlation would provide further evidence of the causal gene.

The RNA-seq data were examined to identify DE genes in the minor effect region outside of the major 877 Kb region, which could be candidates for the minor effect gene. Thirty-nine genes showed DE between pools of susceptible or resistant allele (Supplementary Table S8). *Lsat_1_v5_gn_5_128860* is the only DE gene encoding for an ion channel. Three other DE genes are involved with cell wall integrity, among these are *Lsat_1_v5_gn_5_140040* and *Lsat_1_v5_gn_5_135361*. *Lsat_1_v5_gn_5_140040* encodes a cellulose synthase that is located within a 27.5 Kb deletion in cv. Emperor compared with cv. El Dorado. Some mutants of the ortholog in *Arabidopsis* have reduced cellulose deposition in xylem cell walls (Turner and Somerville 1997) and increased drought and salt tolerance (Chen et al. 2005). It is unclear what effect the deletion in cv. Emperor of *Lsat_1_v5_gn_5_140040* has on tipburn incidence; however, the cell wall could play a role in tipburn incidence by acting as a sink for Ca^{2+} or influencing cellular integrity. *Lsat_1_v5_gn_5_135361* encodes for β -galactosidase 2 (BGAL2), which has been shown to be important in secondary cell wall formation in flax (*Linum usitatissimum*) and hemp (*Cannabis sativa*; Roach et al. 2011 and Behr et al. 2018). However, Moneo-Sánchez et al. (2018) studied knockout mutants of several BGAL genes and found no significant phenotypic changes, which lead them to conclude that other β -galactosidases from the same subfamily can compensate for the loss of function of these proteins.

Only one gene in the minor QTL encodes an ion channel, *Lsat_1_v5_gn_5_128860*. *Lsat_1_v5_gn_5_128860* encodes an ionotropic glutamate receptor-like protein (GLR); ionotropic glutamate receptors are known to play a role in Ca^{2+} flux in rice roots (Ni et al. 2016), root apical meristem cell division at early seedling stage (Li et al. 2006), and lateral root initiation (Vincill et al. 2013). The overexpression of GLRs has been shown to cause symptoms like tipburn in *Arabidopsis* (Kim et al. 2001; Kang et al. 2006). The increased expression of the GLR ortholog in lettuce (*Lsat_1_v5_gn_5_128860*) caused by the cv. Emperor allele does not correlate with increased tipburn incidence. However, the cv. Emperor GLR allele has ~26 insertions, deletions, and substitutions in both exons and introns, thus is likely nonfunctional.

Future studies should investigate recombinants with recombination events in the minor QTL region. To increase the detection

power of differences between lines carrying the susceptible or resistant minor QTL in the experiments, the recombinants should be developed in a background with the susceptible tipburn QTL and the experiments should be conducted in mild climates, such as those experienced in Salinas, CA. In our experiments, these conditions allowed for the greatest detection of the minor QTL.

In our study, *qTPB5.2* fractionated into two QTLs, one of major effect and another of lesser effect. Some, but not all, large effect QTLs in other species have been shown to fractionate into multiple QTLs (Chen and Tanksley 2004; Lecomte et al. 2004; Edwards and Mackay 2009; Studer and Doebley 2011). In tomato, (*Solanum lycopersicum*), QTLs for late blight resistance introgressed from wild tomato species (*Solanum habrochaites*) (Brouwer and St. Clair 2004) were later found to fractionate into multiple QTLs for late blight resistance and other horticultural traits (Johnson et al. 2012; Haggard et al. 2013).

Tipburn is difficult to phenotype reliably due its sensitivity to environmental conditions; therefore, precise molecular markers to assist pyramiding causal genes for resistance would be extremely useful in breeding for improved resistance in the field. Our dissection of *qTPB5.2* is a promising precedent for the dissection and identification of candidate genes at the second major QTL for tipburn located in chromosome 1 (Macias-González et al. 2019). In this study, we narrowed down the location of candidate genes to 877 Kb. Further research is needed to identify the causal genes, but marker EMPxELD_1234_129180 can be immediately used for marker assisted selection to introgress the major resistance allele into new cvs. of iceberg-type lettuce. In addition, two highly resistant homozygous recombinant lines (15G206 and 15G209) with resistant haplotypes for both the major and minor QTLs can be used as the foundation for breeding cvs. with enhanced resistance to tipburn using markers previously identified in scaffolds across the entire QTL (Macias-González et al. 2019). This study also showed that phenotyping for tipburn severity can offer breeders and researchers more power to detect differences for tipburn resistance between lines over tipburn incidence.

Conclusions

We identified candidate genes for the complex physiological trait of tipburn incidence. The initial region of *qTPB5.2* spanned over ~24.5 Mb and 22.8 cM and contained several thousand genes; this was reduced to a region of 877 Kb with major effect on the incidence of tipburn that contained only 12 genes. A second minor effect region is located outside of the major effect region but still within the QTL. Candidate genes include ones encoding proteins associated with cation transport, cellulose synthase, and cell proliferation. These genes are immediately useful as genetic markers for breeding for resistance to tipburn in iceberg lettuce and resistant lines have been developed to introgress the resistant haplotypes of both the major and minor effect regions.

M.M.G. developed and trialed the field experiments, designed RNA-seq experiments, made the crosses to develop recombinant lines, conducted the genotyping of plant material, analyzed the data, interpreted RNA-seq results, designed the follow up studies, and drafted the paper. M.J.T. sequenced the parent lines, designed genetic markers, assisted in experimental design and data interpretation. R.H. conducted the RNA-seq and indel identification analysis. S.J. developed the RIL population. R.W.M. conceived the experiment and assisted in the experimental design, data interpretation, and in writing the paper. All authors have read and approved the final article.

Acknowledgments

Special thanks to Ryan Hayes and Ivan Simko for help in obtaining field space and phenotyping. Thanks to Alexander Kozik for developing Python scripts to process the sequencing data for the recombinants. Thanks to Jose Orozco, German Sandoya, and Lien Bertier for helping in the phenotyping of field experiments. Thanks to Keri Cavanaugh for creating the genomic libraries and for technical assistance in the lab. Thanks to Dean Lavelle for automating the ~1500 DNA extractions with a robot. Thanks to University of Arizona YAC for their help in conducting the experiments in Arizona.

Funding

This work was supported by the California Leafy Greens Research Program and the United States Department of Agriculture, National Institute of Food and Agriculture, Specialty Crop Research Initiative program award numbers 2010-51181-21631 and 2015-51181-24283.

Conflicts of interest

The authors declare that there are no conflicts of interest.

Literature cited

- Altschul SF, Gish W, Miller W, Myers EW, Lipman DJ. 1990. Basic local alignment search tool. *J Mol Biol.* 215:403–410.
- Andrews S. 2010. FastQC: a quality control tool for high throughput sequence data. <http://www.bioinformatics.babraham.ac.uk/projects/fastqc>.
- Barta DJ, Tibbitts TW. 1986. Effects of artificial enclosure of young lettuce *Lactuca sativa* cultivar Buttercrunch leaves on tipburn incidence and leaf calcium concentration. *J Am Soc Hortic Sci.* 111: 413–416.
- Barta DJ, Tibbitts TW. 1991. Calcium localization in lettuce leaves with and without tipburn: comparison of controlled-environment and field-grown plants. *J Am Soc Hortic Sci.* 116:870–875.
- Barta DJ, Tibbitts TW. 2000. Calcium localization and tipburn development in lettuce leaves during early enlargement. *J Am Soc Hortic Sci.* 125:294–298.
- Bates D, Maechler M, Bolker B, Walker S. 2015. Fitting linear mixed-effect models using lme4. *J Stat Softw.* 67:1–48.
- Behr M, Lutts S, Hausman JF, Guerriero G. 2018. Expression analysis of cell wall-related genes in *Cannabis sativa*: the “ins and outs” of hemp stem tissue development. *Fibers.* 6:27.
- Betts MJ, Russell RB. 2003. Amino acid properties and consequences of substitution. In: MR Barnes, IC Gray, editors. *Bioinformatics for Geneticists*. Hoboken, NJ: Wiley.
- Brouwer DJ, St. Clair DA. 2004. Fine mapping of three quantitative trait loci for late blight resistance in tomato using near isogenic lines (NILs) and sub-NILs. *Theor Appl Genet.* 108:628–638.
- Brumm I, Schenk M. 1993. Influence of nitrogen supply on the occurrence of calcium deficiency in field grown lettuce. *Acta Hortic.* 339:125–136.
- Bushnell B. 2014. BMAP: A fast, accurate, splice-aware aligner. <https://www.osti.gov/servlets/purl/1241166>.
- Cantu L, Colombo L, Stoilova T, Demé B, Inouye H, et al. 2017. The A2V mutation as a new tool for hindering A β aggregation: A neutron and x-ray diffraction study. *Sci Rep* 7:5510.
- Chen K-Y, Tanksley SD. 2004. High-resolution mapping and functional analysis of *se2.1*: a major stigma exertion quantitative trait

- locus associated with the evolution from allogamy to autogamy in the genus *Lycopersicon*. *Genetics*. 168:1563–1573.
- Chen M-H, Shao Q-M. 1999. Monte Carlo estimation of Bayesian credible and HPD intervals. *J Comput Graph Stat*. 8:69–92.
- Chen Z, Hong X, Zhang H, Wang Y, Li X, et al. 2005. Disruption of the cellulose synthase gene, *AtCesA8/IRX1*, enhances drought and osmotic stress tolerance in *Arabidopsis*. *Plant J*. 43:273–283.
- Choi K, Lee Y. 2008. Effects of relative humidity on the apparent variability in the incidence of tipburn symptom and distribution of mineral nutrients between morphologically different lettuce (*Lactuca sativa* L.) cultivars. *Hortic Environ Biotechnol*. 49:20–24.
- De Cremer K, Mathys J, Vos C, Froenicke L, Michelmore RW, et al. 2013. RNAseq-based transcriptome analysis of *Lactuca sativa* infected by the fungal necrotroph *Botrytis cinerea*. *Plant Cell Environ*. 36:1992–2007.
- Dobin A, Davis C, Schlesinger F, Drenkow J, Zaleski C, et al. 2013. STAR: Ultrafast universal RNA-seq aligner. *Bioinformatics*. 29:15–21.
- Edwards AC, Mackay TFC. 2009. Quantitative trait loci for aggressive behavior in *Drosophila melanogaster*. *Genetics*. 182:889–897.
- Efroni I, Blum E, Goldshmidt A, Eshed Y. 2008. A protracted and dynamic maturation schedule underlies *Arabidopsis* leaf development. *Plant Cell*. 20:2293–2306.
- Fletcher K, Zhang L, Gil J, Cavanaugh K, Michelmore RW. 2020. AFLAP: Assembly-Free Linkage Analysis Pipeline using k-mers from whole genome sequencing data. *BioRxiv*. doi: 10.1101/2020.09.1.296525.
- Frantz JM, Ritchie G, Cometti NN, Robinson J, Bugbee B. 2004. Exploring the limits of crop productivity: beyond the limits of tipburn in lettuce. *J Am Soc Hortic Sci*. 129:331–338.
- Gasteiger E, Gattiker A, Hoogland C, Ivanyi I, Appel RD, et al. 2003. ExPASy: the proteomics server for in-depth protein knowledge and analysis. *Nucleic Acids Res*. 31:3784–3788.
- Gradstein L, Zolotushko J, Sergeev YV, Lavy I, Narkis G, et al. 2016. Novel GUCY2D mutation causes phenotypic variability of Leber congenital amaurosis in a large kindred. *BMC Med Genet*. 17:52.
- Hadfield JD. 2010. MCMC Methods for multi-response generalized mixed models: The MCMCglmm R package. *J Stat Softw*. 33:1–22.
- Haggard JE, Johnson EB, St. Clair DA. 2013. Linkage relationships among multiple QTL for horticultural traits and late blight (*P. infestans*) resistance on chromosome 5 introgressed from wild tomato *Solanum habrochaites*. *G3 (Bethesda)*. 3:2131–2146.
- Hartz TK, Johnstone PR, Smith RF, Cahn MD. 2007. Soil calcium status unrelated to tipburn of romaine lettuce. *HortScience*. 42:1681–1684.
- Holtzschulze M. 2005. Tipburn in head lettuce: the role of calcium and strategies for preventing the disorder. [Dissertation]. Bonn, Germany: University of Bonn.
- Jackman SD, Vandervalk BP, Mohamadi H, Chu J, Yeo S, et al. 2017. ABySS 2. 0: resource-efficient assembly of large genomes using a bloom filter effect of bloom filter false positive rate. *Genome Res*. 27:768–777.
- Jenni S, Hayes RJ. 2010. Genetic variation, genotype × environment interaction, and selection for tipburn resistance in lettuce in multi-environments. *Euphytica*. 171:427–439.
- Jenni S, Truco M, Michelmore R. 2013. Quantitative trait loci associated with tipburn, heat stress-induced physiological disorders, and maturity traits in crisphead lettuce. *Theor Appl Genet*. 126:3065–3079.
- Johnson EB, Haggard JE, St. Clair DA. 2012. Fractionation, stability, and isolate- specificity of QTL for resistance to *Phytophthora infestans* in cultivated tomato (*Solanum lycopersicum*). *Genes Genomes Genet*. 2:1145–1159.
- Johnson AL, Dirk BS, Coutu M, Haeryfar SMM, Arts EJ, et al. 2016. A highly conserved residue in HIV-1 Nef expression. *mSphere*. 1:1–17.
- Kang S, Kim HB, Lee H, Choi JY, Heu S, et al. 2006. Overexpression in *Arabidopsis* of a plasma membrane-targeting glutamate receptor from small radish increases glutamate-mediated Ca²⁺ influx and delays fungal infection. *Mol Cells*. 21:418–427.
- Kim SA, Kwak JM, Jae SK, Wang MH, Nam HG. 2001. Overexpression of the *AtGluR2* gene encoding an *Arabidopsis* homolog of mammalian glutamate receptors impairs calcium utilization and sensitivity to ionic stress in transgenic plants. *Plant Cell Physiol*. 42:74–84.
- Koyama T, Furutani M, Tasaka M, Ohme-Takagi M. 2007. TCP transcription factors control the morphology of shoot lateral organs via negative regulation of the expression of boundary-specific genes in *Arabidopsis*. *Plant Cell*. 19:473–484.
- Koyama T, Mitsuda N, Seki M, Shinozaki K, Ohme-Takagi M. 2010. TCP transcription factors regulate the activities of ASYMMETRIC LEAVES1 and miR164, as well as the auxin response, during differentiation of leaves in *Arabidopsis*. *Plant Cell*. 22:3574–3588.
- Lecomte L, Saliba-Colombani V, Gautier A, Gomez-Jimenez MC, Duffe P, et al. 2004. Fine mapping of QTLs of chromosome 2 affecting the fruit architecture and composition of tomato. *Mol Breed*. 13:1–14.
- Lenth RV. 2020. emmeans: Estimated marginal means, a.k.a. Last-square means. *J Stat Softw*. 69:1–33. R package version 1.4.4. <http://CRAN.R-project.org/package=emmeans>.
- Li H, Handsaker B, Wysoker A, Fennell T, Ruan J, et al.; 1000 Genome Project Data Processing Subgroup. 2009. The sequence alignment/map format and SAMtools. *Bioinformatics*. 25:2078–2079.
- Li J, Zhu S, Song X, Shen Y, Chen H, et al. 2006. A rice glutamate receptor-like gene is critical for the division and survival of individual cells in the root apical meristem. *Plant Cell*. 18:340–349.
- Li P, Zhang G, Gonzales N, Guo Y, Hu H, et al. 2016. Ca²⁺-regulated and diurnal rhythm-regulated Na⁺/Ca²⁺ exchanger AtNCL affects flowering time and auxin signalling in *Arabidopsis*. *Plant Cell Environ*. 39:377–392.
- Livingstone CD, Barton CJ. 1993. Protein sequence alignments: a strategy for the hierarchical analysis of sequence conservation. *Comput Appl Biosci*. 9:745–756.
- Macias-González M, Truco MJ, Bertier LD, Jenni S, Simko I, et al. 2019. Genetic architecture of tipburn in lettuce. *Theor Appl Genet*. 132:2209–2222.
- Macias-González M, Truco MJ, Smith R, Cahn M, Simko I, et al. 2020. Genetics of robustness under nitrogen and water deficient conditions in field grown lettuce. *Crop Sci*. 1–78. doi: 10.1002/csc2.20380.
- Marçais G, Kingsford C. 2011. A fast, lock-free approach for efficient parallel counting of occurrences of k-mers. *Bioinformatics*. 27:764–770.
- McCarthy DJ, Chen Y, Smyth GK. 2012. Differential expression analysis of multifactor RNA-seq experiments with respect to biological variation. *Nucleic Acids Res*. 40:4288–4297.
- Misaghi IJ, Grogan RG. 1978. Effect of temperature on tipburn development in head lettuce. *Phytopathology*. 68:1738–1743.
- Moneo-Sánchez M, Izquierdo L, Martín I, Hernández-Nistal J, Albornos L, et al. 2018. Knockout mutants of *Arabidopsis thaliana* β-galactosidase. Modifications in the cell wall saccharides and enzymatic activities. *Biologia Plant*. 62:80–88.
- Nag A, King S, Jack T. 2009. miR319a targeting of TCP4 is critical for petal growth and development in *Arabidopsis*. *Proc Natl Acad Sci U S A*. 106:22534–22539.

- Nath U, Crawford BCW, Carpenter R, Coen E. 2003. Genetic control of surface curvature. *Science*. 299:1404–1407.
- Ni J, Yu Z, Du G, Zhang Y, Taylor JL, et al. 2016. Heterologous expression and functional analysis of rice GLUTAMATE RECEPTOR-LIKE family indicates its role in glutamate triggered calcium flux in rice roots. *Rice (N. Y.)*. 9:9–14.
- Nicolas M, Cubas P. 2016. TCP factors: New kids on the signaling block. *Curr Opin Plant Biol*. 33:33–41.
- Olle M, Bender I. 2009. Causes and control of calcium deficiency disorders in vegetables: a review. *J Hort Sci Biotechnol*. 84:577–584.
- Palatnik JF, Allen E, Wu X, Schommer C, Schwab R, et al. 2003. Control of leaf morphogenesis by microRNAs. *Nature*. 425:257–263.
- Plummer M. 2006. CODA: Convergence diagnosis and output analysis for. *MCMC R News*. 6:7–11.
- Quinlan AR, Hall IM. 2010. BEDTools: a flexible suite of utilities for comparing genomic features. *Bioinformatics*. 26:841–842.
- R Core Team 2019. R: A Language and Environment for Statistical Computing. Vienna, Australia: R Foundation for Statistical Computing. <https://www.r-project.org/>.
- Reyes-Chin-Wo S, Wang Z, Yang X, Kozik A, Arikiti S, et al. 2017. Genome assembly with in vitro proximity ligation data and whole-genome triplication in lettuce. *Nat. Commun*. 8:14953.
- Roach MJ, Mokshina NY, Badhan A, Snegireva AV, Hobson N, et al. 2011. Development of cellulosic secondary walls in flax fibers requires β -galactosidase. *Plant Physiol*. 156:1351–1363.
- Robinson MD, McCarthy DJ, Smyth GK. 2010. edgeR: A bioconductor package for differential expression analysis of digital gene expression data. *Bioinformatics*. 26:139–140.
- Rodriguez RE, Mecchia MA, Debernardi JM, Schommer C, Weigel D, et al. 2010. Control of cell proliferation in *Arabidopsis thaliana* by microRNA miR396. *Development*. 137:103–112.
- Ryder EJ, Waycott W. 1998. Crisphead lettuce resistant to tipburn: cultivar Tiber and eight breeding lines. *HortScience*. 33:903–904.
- Sarvepalli K, Nath U. 2011a. Interaction of TCP4-mediated growth module with phytohormones. *Plant Signal Behav*. 6:1440–1443.
- Sarvepalli K, Nath U. 2011b. Hyper-activation of the TCP4 transcription factor in *Arabidopsis thaliana* accelerates multiple aspects of plant maturation. *Plant J*. 67:595–607.
- Schommer C, Debernardi JM, Bresso EG, Rodriguez RE, Palatnik JF. 2014. Repression of cell proliferation by miR319-regulated TCP4. *Mol Plant*. 7:1533–1544.
- Seki K, Komatsu K, Tanaka K, Hiraga M, Kajiyama-Kanegae H, et al. 2020. A CIN-like TCP transcription factor (*LsTCP4*) having retrotransposon insertion associates with a shift from Salinas type to Empire type in crisphead lettuce (*Lactuca sativa* L.). *Hortic Res*. 7:15.
- Stoffel K, van Leeuwen H, Kozik A, Caldwell D, Ashrafi H, et al. 2012. Development and application of a 6.5 million feature Affymetrix Genechip® for massively parallel discovery of single position polymorphisms in lettuce (*Lactuca spp.*). *BMC Genomics*. 13:185.
- Studer AJ, Doebley JF. 2011. Do large effect QTL fractionate? A case study at the maize domestication QTL teosinte branched1. *Genetics*. 188:673–681.
- Truco MJ, Antonise R, Lavelle D, Ochoa O, Kozik A, et al. 2007. A high-density, integrated genetic linkage map of lettuce (*Lactuca spp.*). *Theor Appl Genet*. 115:735–746.
- Truco MJ, Ashrafi H, Kozik A, van Leeuwen H, Bowers J, et al. 2013. An ultra high-density, transcript-based, genetic map of lettuce. *G3 (Bethesda)*. 3:617–631.
- Turner SR, Somerville CR. 1997. Collapsed xylem phenotype of *Arabidopsis* identifies mutants deficient in cellulose deposition in the secondary cell wall. *Plant Cell*. 9:689–701.
- Vincill ED, Clarin AE, Molenda JN, Spalding EP. 2013. Interacting glutamate receptor-like proteins in phloem regulate lateral root initiation in *Arabidopsis*. *Plant Cell*. 25:1304–1313.
- Wang P, Li Z, Wei J, Zhao Z, Sun D, et al. 2012. A $\text{Na}^+/\text{Ca}^{2+}$ exchanger-like protein (*AtNCL*) involved in salt stress in *Arabidopsis*. *J Biol Chem*. 287:44062–44070.
- Zhong S, Joung JG, Zheng Y, Chen YR, Liu B. 2011. High-throughput illumina strand-specific RNA sequencing library preparation. *Cold Spring Harb Protoc*. 6:940–949.

Communicating editor: R. Wisser